Electrochemical characterization of a unique, "neutral" laccase from Flammulina velutipes

doi: 10.1016/j.jbiosc.2012.09.011

Electrochemical characterization of a unique, “neutral” laccase from *Flammulina velutipes*

Kaori (Otsuka) Saito[a], Shinji Kurose[b], Yoshio Tsujino[c*], Toshiyuki Osakai[d], Kunishige Kataoka[b], Takeshi Sakurai[b], Eiichi Tamiya[e]

[a] *School of Materials Science, Japan Advanced Institute of Science and Technology, 1-1, Asahidai, Nomi, Ishikawa 923-1292, Japan*

[b] *Graduate school of Natural Science and Technology, Kanazawa University, Kakuma, Kanazawa, 920-1192, Japan*

[c] *Laboratory for Cosmetic Science, Faculty of Pharmaceutical Sciences, Chiba Institute of Science, 15-8, Shiomi, Choshi, 288-0025, Japan*

[d] *Department of Chemistry, Graduate School of Science, Kobe University, Nada, Kobe 657-8501, Japan*

[e] *Department of Applied Physics, Graduate School of Engineering, Osaka University, 2-1, Yamadaoka, Suita, 565-0871, Japan*

Short title: *Electrochemical consideration on the oprimum pH of laccase*

[*] Corresponding author. Tel.: +81-(0)80-3629-3343; fax: +81-(0)78-441-4780

E-mail address: ytsujino@cis.ac.jp (Y. Tsujino)

Category for listing: enzymatic assays and analyses

Abstract

The *flac1* gene consisted of 1,488 bases encodes a novel laccase (Flac1) from *Flammulina velutipes*. The deduced amino acid sequence of Flac1 with 496 amino acids shows 58–64% homologies with other fungal laccases. The recombinant Flac1 (rFlac1) was heterologously expressed in *Pichia pastoris*, with sugars of ca. 4 kDa attached on the protein molecule, which has the calculated molecular mass of 53,532 Da. rFlac1 was shown to be a multi-copper oxidase from spectroscopies. The optimum pHs of rFlac1 for oxidations of 2,2'-azino-bis(3-ethylbenzothiazoline-6-sulfonic acid), *p*-phenylenediamine, and *o*-aminophenol, were 5.0, 5.0, and 6.0–6.5, respectively, showing higher pH values than those from many other fungal laccases. The slightly acidic or neutral optimum pH that is not strongly dependent on substrates is a unique property of rFlac1. Effective O_2 reduction was realized by the direct electron transfer of rFlac1 at a highly oriented pyrolytic graphite electrode modified with fine carbon particles (Ketjen Black) in O_2-saturated solution. The pHs showing the maximum $\Delta E^{\circ\prime}$ (= $E^{\circ\prime}$(enzyme) – $E^{\circ\prime}$(substrate)) coincided well with the optimum pHs shown by rFlac1 under steady-state conditions. The present electrochemical results of rFlac1 indicate that $\Delta E^{\circ\prime}$ is one of the primary factors to determine the activity of multi-copper oxidases.

Keywords: Laccase; *Flammulina velutipes*; Heterologous expression; Direct electron transfer; Redox potential; Optimum pH

Introduction

Multi-copper oxidases, including laccase (EC 1.10.3.2) and bilirubin oxidase (BOD, EC 1.3.3.5) catalyze oxidations of various aromatic and some inorganic compounds with the concomitant reduction of O_2 to water (1). Their wide range of substrate specificities, the use of dioxygen as the second substrate, and no production of activated oxygen species suggest possible industrial applications, such as delignification of Kraft pulp, coloring and bleaching of textiles, oxidative degradation of organic pollutants, and the development of biosensors and biofuel cells. Multi-copper oxidases contain four coppers classified into three types, type 1, type 2, and type 3, according to their spectroscopic and magnetic properties. The catalytic reaction of a multi-copper oxidase involves [1] the reduction of the type 1 copper with substrate, [2] intramolecular long-range electron transfer (ET) [1] from the type 1 copper to the type 2 and type 3 coppers, which form a trinuclear copper cluster, and [3] the reduction of O_2 to water at the trinuclear copper cluster. It is well known that the optimum pH of multi-copper oxidases change depending on both redox properties of their copper centers and substrate. Based on the pattern of the optimum pHs for different substrates, i.e., 2,2'-azino-bis-(3-ethylbenzothiazoline-6-sulfonic acid) (ABTS) and phenols, laccases are classified into four groups, as described as follows: The first group from *Polyporus pinsitus* (2) and *Lentinula edodes* (3) to show the highest oxidation activity at acidic pHs for both ABTS and phenols, the second group from *Panaeolus sphinctrinus* (2), *Melanocarpus albomyces* (4), *Rhizoctonia solani* (5), and *Pleurotus ostreatus* (6) to show the highest activity at acidic and neutral pHs for ABTS and phenols, respectively,

the third group from *Phellinus ribis* (7) to show the highest activity at neutral pH for both substrates, and the fourth group from *Coprinus friesii* (2) to show the highest activity at neutral and alkaline pHs for ABTS and phenols, respectively. Although laccases have been isolated from various fungi, plants, and insects, laccases with a high activity under neutral or alkaline conditions are limited (2,8,9).

The optimum pH of multi-copper oxidase depends on the natures of the enzyme and substrate. Ascending and descending branches of the bell-shaped pH–activity curve are derived from properties of the enzyme itself including deformation of the protein structure. In addition to these inherent effects originated in the enzyme, however, a contribution from the properties of substrate to the pH–activity profile is not also negligible in the reaction of multi-copper oxidase. This is presumably because the ET rate from substrate to enzyme (type 1 copper site) is the initial step of a series of enzymatic processes of multi-copper oxidases. The difference of the redox potential between substrate and type 1 copper determines the rate for this intermolecular process of multi-copper oxidases.

The redox potential of the type 1 copper site of multi-copper oxidases has been determined with a redox titration method under anaerobic conditions by monitoring the absorption changes at ca. 600 nm. However, the method requires a large amount of enzyme and it have to be kept under rigorous anaerobic conditions for a long time. Therefore, there have been only a few reports on the pH dependence of the redox potential of multi-copper oxidases (10,11). Further, the use of one or more electron mediators might affect the redox property of the enzyme. Recently, however, the direct

electron transfer (DET) of multi-copper oxidases has been reported by Kano et al. (12), Tsujimura et al. (13), and Shleev et al. (14-16). The DET of a bilirubin oxidase has been studied in detail using a highly oriented pyrolytic graphite (HOPG) electrode, and the obtained steady-state current–potential curves could be theoretically analyzed to obtain thermodynamic and kinetic parameters for the DET reaction (13). We have performed the analogous electrochemical and kinetic analyses of BOD under different pH conditions (17). The obtained formal redox potential, $E^{\circ\prime}$, of BOD was almost constant in the pH range of 2.0–5.5, slightly shifting to negative potentials with increasing pH. The pH dependences of $E^{\circ\prime}$ of substrates such as *p*-phenylenediamine (PPD), *o*-aminophenol (OAP), and ABTS were also studied, and it was then found that the pH range showing the maximum $\Delta E^{\circ\prime}$ value ($E^{\circ\prime}$(BOD)–$E^{\circ\prime}$(substrates)) corresponds well with the optimum pHs of BOD for the respective substrates. It has thus been suggested that $\Delta E^{\circ\prime}$ is a useful indicator of the enzymatic activity of BOD (17). However, other factors such as protein structure, stability, and affinity to substrates, may also contribute to the pH–activity relationship of multi-copper oxidases. To elucidate how multi-copper oxidases give the pH optima at higher pHs, profound studies on laccases and related enzymes showing high activities at neutral to alkaline pHs are required.

Recently, we found a unique laccase Flac1, in the culture supernatant of *Flammulina velutipes*, which has the optimum pHs in a slightly acidic or neutral region (pH 5.0–6.5) depending sparingly on substrates (i.e., ABTS, PPD, OAP, 2,6-dimethoxyphenol (DMP), syringaldazine (SGZ)) (18). Laccases, which show high activity at pH range from neutral to alkaline conditions and preferably show a steady

optimum pH for a variety of substrates are strongly required for wider industrial applications. In this study, we cloned and constructed the heterologous expression system of the gene coding for this novel laccase, Flac1, in *Pichia pastoris*. On analyzing the redox properties of rFlac1 by DET, the origin of the "neutral" optimum pH was discussed in terms of redox potentials of the enzyme and substrates.

Materials and methods

Strains and chemicals

F. velutipes NBRC 30601 was purchased from National Institute of Technology and Evaluation (Japan). *P. pastoris* GS115, the Multi-copy *Pichia* Expression Kit and cultivation medium were from Invitrogen, and *Escherichia coli* XL10 GOLD from Stratagene. The designed oligonucleotides were purchased from BEX (Japan). All other chemicals were of analytical grade and purchased from Wako Pure Chemical Industries, Ltd. (Japan).

cDNA cloning and sequence determination

The mycelia of *F. velutipes* were frozen in liquid nitrogen and gently ground in a mortar with a pestle under cooling with liquid nitrogen. mRNA was extracted from the cell powder using Dynabeeds mRNA Direct Kit (Dynal). Reverse transcription was performed according to the manufacturer's instruction manual using First Strand cDNA Synthesis Kit (Amersham Bioscience).

In order to obtain the Flac1 gene (*flac1*), we designed the sense primer (Flac1-N: 5'-ggnatyggiccnathac-3') based on the N-terminal amino acid sequence of the mature Flac1, GIGPTDLVIANADVAPDGF, and the antisense primer (WRF-1R: 5'-rtggcartgsagraa-3') including the amino acid sequence conserved in laccases from white-rot fungi, His-Cys-His near the C-terminal end.

The 1,350 bp fragment of *flac1* was amplified by PCR using above two primers and the cDNA library as template and cloned into pGEM-T easy vector (Promega) and the resultant vector was named pGEM-Flac1-5. The 3'-terminal region of *flac1* (700 bp) was acquired using Flac1-1 (5'-tttgcctgctggttc-3'), a primer designed based on the sequence of *flac1* fragment and *Not*I-d$(T)_{18}$ primer (Amersham Bioscience) and the cDNA library as template. The fragment was ligated into pGEM-Flac1-5 to yield the complete cDNA fragment of *flac1* and the resultant plasmid was named pGEM-Flac1. The DNA sequencing of *flac1* was performed using Thermo Sequenase Primer Cycle Sequencing Kit (Amersham Bioscience) on a DNA Sequencer (Hitachi SQ5500E).

Expression of flac1 in P. pastoris

In order to construct the expression plasmid containing the gene encoded the secretion signal sequence of the *Pleurotus sajor-caju* laccase-4, three overlapping oligonucleotides were designed based on the sequence of 23 residues, *P. sajor-caju* laccase-4 signal sequence (MFPGARILATLTLALHLLHGTHA). A 97-bp gene fragment consisting of the *Eco*RI linker (underline), the laccase-4 signal coding

sequence, and the 5’-region of flac1 was synthesized by PCR using the following primers.

Flac-ple-sig1: 5’ gaattcaccatggttccaggcgcacggattcttgctacgcttaccttggccct 3’

Flac-ple-sig1R: 5’ atagcagcatgagtcccatgcaaaagatgaagggccaaggtaagcgtagc 3’

Flac-ple-sig2: 5’ catgggactcatgctgctattgggccaataacgg 3’

The about 0.7-kbp PCR fragment formed using this gene fragment and Flac1-1R: 5’-cagacggaaacgatatcg-3’, antisense primer annealed 3’-downstream region of the internal *Eco*RI site of flac1, as primers and pGEM-Flac1 as template were digested with *Eco*RI and cloned into pPIC3.5k with 0.9-kbp *flac1* fragment digested with *Eco*RI and *Not*I to yield pPIC3.5-Flac1. The resultant expression plasmid contains the *flac1* gene under the control of the AOX1 promoter.

The competent cells of *P. pastoris* GS115 were transformed by electroporation with pPIC3.5-Flac1 linearized with *Mss*I. The transformants with laccase activity were screened by activity-staining on a Buffered Minimal Methanol (BMM, 100 mM potassium phosphate (pH 6.0), 1.34% yeast nitrogen base, 4×10^{-5}% biotin, 2.0% D-glucose, and 0.5% methanol) agar plate containing 1 mM ABTS at 30 °C. Methanol was added on the lid of petri dish every day. After a few days, circumferences of the positive colonies turned green.

Purification of the recombinant Flac1 (rFlac1)

Cultivation of transformants was performed as in the expression of BOD (19). The culture supernatant (6.4 L) was collected by centrifugation and $(NH_4)_2SO_4$ was

added to 25% degree of saturation. The supernatant was adsorbed on a TOYOPEARL Butyl-650M column (ϕ5 × 20 cm), and was eluted with 25%→0% saturated $(NH_4)_2SO_4$ gradient. The fractions with laccase activity were collected and dialyzed with 50 mM Tris-H_2SO_4 (pH 8.5). Fractions with activity on a TOYOPEAL DEAE-650M column (ϕ2.5 × 30 cm), which was pre-equilibrated with the same buffer and eluted with 0.1→0.4 M Na_2SO_4 gradient, were collected and pooled. Protein concentration was determined using a BCA (bicinchoninic acid) protein assay reagent (Pierce) and from the absorption intensity at 280 nm, ε = 57.2 $mM^{-1}\cdot cm^{-1}$. Deviations in the two independent methods were less than 5%.

Enzyme Activities

Laccase activity for oxidations of DMP, ABTS, and PPD were spectroscopically determined by monitoring the absorption changes at 470 nm (ε = 36.5 $mM^{-1}\cdot cm^{-1}$), 420 nm (ε = 36.0 $mM^{-1}\cdot cm^{-1}$), and 487 nm (ε = 14.7 $mM^{-1}\cdot cm^{-1}$), respectively, in the acetate buffer, pH 5.5. The final concentration of the buffer and substrate were 0.18 M and 5 mM, respectively. One unit was defined as the amount of enzyme that oxidized 1 μmol of substrate per minute. For OAP, 1 unit was defined as the amount of enzyme that increases 1 absorbance value at 420 nm per minute. Optimum pHs were determined by monitoring the oxidations of ABTS, PPD, and OAP in the MES-Tris-sodium acetate buffer. ABTS and PPD were dissolved in water, whereas OAP was dissolved in dimethylsulfoxide (DMSO) and then water was added until the DMSO concentration became 10%.

Measurements of absorption, CD, ESR, and atomic absorption spectra

Absorption spectra were measured on a JASCO Ubest 50 spectrometer and circular dichroism (CD) spectra on a JASCO J-500C spectropolarimeter. X-band electron spin resonance (ESR) spectra were recorded on a JEOL JES-REIX spectrometer at 77 K. The total copper amount in rFlac1 was determined by atomic absorption spectroscopy on a Varian SpectrAA-50 spectrometer.

Cyclic voltammetry

Cyclic voltammetry (CV) was performed using a potentiostat (model HA10100mM1A, Hokuto Denko Co., Japan) operating in the three-electrode mode. For the CV measurements of Flac1, a highly oriented pyrolytic graphite (HOPG) electrode with the roughness of the electrode surface (geometric area, 0.28 cm^2) being increased by modification of Ketjen Black (KB, EC 300J) as an enzyme-adsorbing electroconductive material was used. For modification of the HOPG electrode, polyvinylidene difluoride (PVDF, Aldrich) was dissolved in *N*-metyl-2-pyrrolidone (NMP) to prepare a 10% (w/w) solution. KB powder, which was ground in advance with an agate triturator, was mixed with the PVDF solution (80:20, w/w) to prepare KB slurry. NMP (50 μl) was added to the KB slurry (10 mg), and then the mixture (1–2 μl) was applied to the surface of the electrode. The electrode was dried in a drying oven at 60 °C for 12 h. The KB-modified HOPG electrode was immersed into Flac1 solution (12 μM) for 2 h at 4 °C, and then CV measurements were performed in a 0.1 M Britton

& Robinson (BR) buffer. A Pt coil electrode and a Ag|AgCl|$KCl_{sat.}$ electrode were used as the counter and reference electrodes, respectively. The test solution was saturated with oxygen by bubbling with oxygen gas (99.5%) for 10 min.

Results and discussion

Amino acid sequence of Flac1

Fig. 1A shows the cDNA sequence of *flac1*, in which the region encoding the possible pre- and pro- sequences were deleted (accession number for the GenBank, AB253791). The *flac1* consisting of the 1,488 bases encodes the mature protein of Flac1, which consists of 496 amino acids and has 53,532 Da molecular mass. Homologies of the amino acid sequence of Flac1 with fungal laccases from *Trametes versicolor*, *Coriolus hirsutus*, *Pleurotus ostreatus*, and *Coprinus cinereus* were as high as 63, 58, 64, and 61%, respectively, while those with other multi-copper oxidases, plant laccases from *Rhus vernicifera* (20), ascorbate oxidase from zucchini (21), and BOD from *Myrothecium verrucaria* (22) were 25, 28, and 21%, respectively (partial amino acid sequence alignment of multi-copper oxidases shown in Fig. 1B). Although multi-copper oxidases with high phenol oxidase activities has been classified into laccases regardless of its origin, plants, fungi, or insects, Flac1 apparently belongs to fungal laccase branch from amino acid sequence and phylogenic tree (not shown).

As for the protein structure, Flac1 consists of three cupredoxin domains similarly to many other multi-copper oxidases (23). Based on the amino acid sequences

and crystal structures of *Trametes versicolor* and *Coprinus cinereus* laccases (24,25), it has been supposed that two disulphide bonds are formed between Cys85-Cys485 and Cys117-Cys213 as indicated in Fig. 1. Only one *N*-glycosylation site is present at Asn434 (Asn-Val-Thr) (26), but it is not certain whether the site is glycosylated or not in the authentic Flac1. Further, there is no information about the presence or absence of the *O*-glycosylation site in the authentic Flac1.

The amino acids coordinating each type of copper ion are identified from the sequence alignment. His395, His457, and Cys452 are the ligands for type 1 copper. Differing from many other multi-copper oxidases, fungal laccases do not have the fourth ligand, Met, and the non-coordinating amino acid, Leu or Phe occupies the corresponding position, giving a high redox potential to type 1 copper (27). Leu462 corresponds to this amino acid in Flac1. Ligands for type 2 copper are His64 and His398, and a water molecule or hydroxide ion is the third ligand for this copper. Ligands for one of type 3 coppers are His66, His109, and His453, and those for another type 3 copper are His111, His400, and His451, as judged from the sequence alignment. A hydroxide group bridges between type 3 coppers, making them ESR-undetectable in the resting state. All copper sites are closely connected each other through the peptide backbone (28).

Expression of rFlac1

We constructed the heterologous expression system of Flac1 using *P. pastoris*, which has been used as one of excellent hosts to express laccase and other multi-copper

oxidases (29,30), because high-level expression is attainable due to multicopying the target gene under the control of the AOX1 gene promoter. *P. pastoris* GS115 transformed with pPIC3.5-Flac1 with the signal sequence of *P. sajor-caju* laccase-4 showed laccase activity in culture supernatant, whereas the α-factor secretion signal of *Saccharomyces cerevisiae* did not function to secret rFlac1 outside *P. pastoris* (data not shown).

Purification and characterizations of rFlac1

rFlac1 was purified by hydrophobic (TOYOPEARL Buthyl-650) and anion exchange (TOYOPEARL DEAE-650) chromatographies (Table S1). The final yield of rFlac1 was 50%. SDS-PAGE gave a single band at 57.8 kDa (Fig. S1). Gel filtration chromatography indicated that rFLac1 is monomeric. Because the calculated molecular mass was 54 kDa, however, the difference in ca. 4 kDa will be due to an attaching of sugars on the protein surface by *P. pastoris* (one *N*-glycosylation site was identified from amino acid sequence (*vide supra*)).

The absorption spectrum of rFlac1 at pH 7.0 (Fig. 2A) shows the strong band at 600 nm derived from the $Cys(S^-)_\pi \rightarrow Cu^{2+}$ (Type 1 copper) charge transfer. Its molar extinction coefficient is 2700 M^{-1} cm^{-1}, the value smaller than those of other multi-copper oxidases (ca. 4000 – 6000), indicating that appreciable amounts of apo-proteins are present (*vide infra*). The absorption band at around 750 nm comes from the d-d absorption of type 1 copper. The shoulder band at around 330 nm was derived from the paired type 3 coppers, supporting that the trinuclear copper center was

properly constructed in rFlac1 (1). Although the yield of rFlac1 was not very high, the absorption spectrum of Flac1 was obtained for the first time.

The CD spectrum of rFlac1 is shown in Fig. 2B. The negatively signed band at 620 nm and the positively signed band at 510 nm come from the charge transfers, $Cys(S^-)_\pi \rightarrow Cu^{2+}$ and $Cys(S^-)_\sigma \rightarrow Cu^{2+}$, respectively. While the sign of the former band was reverted from those of the plant laccase, ascorbate oxidase, and BOD (31,32), the total number of bands and their wavelengths were very similar to those of the fungal laccases reported previously (1). The positively signed band at 370 nm and the negatively signed band at 455 nm were derived from the charge transfers $His(N) \rightarrow Cu^{2+}$. The positively signed weak band at 760 nm was originated in the d-d transitions of Cu^{2+} ions. All these bands were dominantly derived from type 1 copper and the contributions from other types of copper were masked by the bands appeared in the near-UV to visible regions except the negatively signed small band at 330 nm derived from type 3 coppers. The intensity of this band due to the charge transfer $OH^- \rightarrow Cu^{2+}$ was weak compared to its intensity in the absorption spectrum (Fig. 2A), because the band was concerned with the exogenous OH^- group to bridge between type 3 coppers.

The ESR spectrum of rFlac1 is shown in Fig. 2C. The signals derived from type 1 and type 2 coppers are clearly observed with equal intensities. Their spin Hamiltonian parameters are $g_{//} = 2.23$ and $A_{//} = 9.23 \times 10^{-3}$ cm^{-1} for type 1 copper and $g_{//} = 2.23$ and $A_{//} = 18.8 \times 10^{-3}$ cm^{-1} for type 2 copper. Analogous parameters have been reported for fungal laccases (1). Type 3 coppers were not detected, supporting that they were antiferromagnetically coupled as in other multi-copper oxidases.

The copper content in rFlac1 was determined to be 2.0 per protein molecule by atomic absorption spectroscopy. Copper ions deeply buried inside the protein molecule may not be atomized fully, and this might have led to smaller copper contents than the expected values as have frequently been reported for large sized copper-protein molecules. However, the presence of apo-proteins has been frequently reported in the expressions of laccases and bilirubin oxidase (33). If the presence of apo-protein by ca. 50% is anticipated, the molar extinction coefficient becomes 5,400, the normal value reported for type 1 copper, and intensities of the CD bands also approach the values reported for holo-multi-copper oxidases (34). Apparent enzymatic activities (Table 1,S1 and Fig. 2-5) and all spectral properties (Fig. 2) exclude a random incorporation of copper ions into protein molecule.

Optimum pH of rFlac1

The pH dependence of the activities of rFlac1 for the oxidations of ABTS, PPD, and OAP are shown in Fig. 3. The optimum pH was 5.0, 5.0, and 6.0–6.5 for ABTS, PPD, and OAP, respectively. These results correspond well to those of the authentic Flac1 (18), ensuring the successful expression of rFlac1. The specific activity of rFlac1 at optimum pH was determined as 54.7, 16.1, and 627 U/mg for ABTS, PPD, and OAP, respectively. For ABTS and PPD, 1 unit was defined as the amount of enzyme that oxidizes 1 μmol of substrate per minute. There is no reliable data of the molar extinction coefficient value of OAP, therefore 1 unit was defined as the amount of enzyme that increases 1 absorbance value at 420 nm per minute. The reason why these

pH profiles of activities for each substrate does not coincide with those of $\Delta E^{o\prime}$ (*vide infra*) will be that absorption spectroscopy does not exclusively follow formations of the initial products after one-electron oxidation. In addition, a turnover of rFlac1 involves many steps such as the electron transfer from substrate to type 1 copper, the long range intramolecular electron transfer from type 1 copper to the trinuclear copper center comprised of a type 2 copper and a pair of type 3 coppers, at which the reduction of a dioxygen molecule takes place using four protons to produce two water molecules depending on pH (35, 36).

Electrochemical O_2 reduction by rFlac1

It was difficult to obtain a wave for the DET-type rFlac1-catalyzed O_2 reduction at an unmodified HOPG electrode (data not shown). This is probably due to the low surface concentration of enzyme and/or the low ET ability between the enzyme and the electrode surface. Recently, a high current density (10 mA cm^{-1}) was successfully obtained for the DET of D-fructose dehydrogenase by using a modified electrode on its surface with fine carbon particles "Ketjen Black (KB)" (37). In accordance with the report, the DET of rFlac1 could be realized on a KB modified HOPG electrode. When the electrode potential was swept from 0.7 V to 0.0 V at the scan rate of 0.02 V s^{-1}, a relatively large charging current of ca. 100 μA cm^{-2} was observed at the bare KB modified HOPG electrode in an O_2-saturated BR buffer of pH 5.0 (Fig. 4A, line b). By immersing the electrode into an rFlac1 solution for 2 h, rFlac1 was adsorbed at the electrode surface, and then gave a well-developed reduction wave

at around 0.6 V (Fig. 4A, line a). This wave is considered to be due to the reduction of O_2 catalyzed by rFlac1 absorbed on the electrode, since the wave was not observed in the buffer bubbled with nitrogen gas instead of oxygen gas. It seems that the enzymes are not absorbed on the electrode in a direction-specific manner, and accordingly, only a definite portion of the absorbed enzymes are able to undergo ET with the electrode through the type 1 copper site. A portion of such effectively oriented enzymes is presumably small for the HOPG electrode that is not modified with KB. At the HOPG electrode modified with fine particles of KB, however, the enzyme molecules may be efficiently adsorbed on the electrode surface so that the population of type 1 copper site oriented the electrode surface would be increased, affording a clear catalytic current.

Since the observed current for rFlac1 was hardly affected by the scan rate in the range of 0.012 to 0.025 V s^{-1} (data not shown), the current is considered as due to the enzyme-catalyzed O_2 reduction. To perform the quantitative analysis of the catalytic current, however, we had to subtract the base current. As shown in Fig. 4A, the non-faradic current around 0.6 V was somewhat decreased by the adsorption of rFlac1 on the electrode. Then, the base current was corrected for the effect of enzyme adsorption by multiplying the measured current with an appropriate factor of ~0.8, which was determined so that the currents at ~0.6 V coincided with each other in the presence and absence of the enzyme.

The cyclic voltammograms for the DET of rFlac1 under different pH conditions are exemplified in Fig. 4C. Well-defined DET currents could be obtained in a wide pH range of 2.0 to 7.0, although the current density was very low at pH higher

than 7.5 (data not shown). The maximum current density was obtained at pH 5.0. The potential to give the cathodic wave was pH-dependent.

It was previously reported that the current density (i) for a DET-type catalytic O_2 reduction wave for BOD should be expressed by the following equation (13)

$$i = \frac{nFk_c\Gamma_t}{1 + (k_c / k_f) + (k_b / k_f)} \qquad (1)$$

where n, F, and Γ_t are the number of electrons (n = 1 for the type 1 copper in BOD), the Faraday constant, and the total surface concentration of the enzyme, respectively. The catalytic constant, k_c, includes the intramolecular ET rate constant from type 1 copper to type 2/type 3 coppers and the intermolecular ET rate constant for the O_2 reduction at the type 2/type 3 copper cluster. The k_f and k_b values are the forward and backward ET rate constants between electrode and enzymes, respectively, and are assumed to be expressed by the following Butler–Volmer-type equations:

$$k_f = k^{\circ\prime}\exp\left[-\alpha(nF/RT)(E - E^{\circ\prime})\right] \qquad (2)$$

$$k_b = k^{\circ\prime}\exp\left[(1-\alpha)(nF/RT)(E - E^{\circ\prime})\right] \qquad (3)$$

where $E^{\circ\prime}$, k°, and α are the formal potential of the type 1 copper site in BOD, the standard surface ET rate constant, and the transfer coefficient, respectively. Tsujimura et al. performed a non-linear regression analysis of the bulk electrolysis of BOD by using the above equations with the $E^{\circ\prime}$ value of 0.460 V (at pH 7.0) (13). In this work, however, $E^{\circ\prime}$ was treated as an adjusting parameter as well as k°, Γ_t, and α, because $E^{\circ\prime}$ should be considered rigorously for the surface redox reaction (17). Since there is no relevant data, the k_c value was assumed to be 250 s^{-1}, the value for BOD (13).

Intrinsically, k_c should be dependent on pH, however, when the k_c value was changed largely from 250 s^{-1}, the regression analysis was not successful. The "onset" potential, at which the cathodic waves appear in the fitting curves, is not governed by the k_c value, although it significantly affects the current density of the fitting curves. The onset potential was governed mostly by the value of $E°'$. A representative catalytic wave obtained after subtraction of the corrected base current is shown in Fig. 4B. As seen in the figure, the "steady-state" currents recorded on the forward (cathodic) and backward (anodic) scans differed considerably. Though the origin has not been clarified yet, the current on the forward scan was analyzed according to a conventional manner.

Using a non-linear regression analysis program (Excel®), the base current-corrected catalytic waves recorded on the cathodic scan were curve-fitted by using Eq. (1) with Eqs. (2) and (3). As exemplified in Fig. 5A, the experimental current–potential curves could be well reproduced in the pH range of 2.0–7.0. The precision of the fitting analysis was estimated from the standard deviation:

$$\sigma = \left[\sum \left(i_{\mathrm{calcd}} - i_{\mathrm{obsd}}\right)^2 / \left(N - 1\right)\right]^{1/2} \qquad (4)$$

where i_{calcd} and i_{obsd} are the calculated and observed current densities, respectively. Table 1 shows the values of $k°$, α, Γ_t, $E°'$, and σ obtained from the regression analysis. The value of σ ranged from 1.0 to 2.6 μA cm^{-2}.

The pH dependence of $E°'$ of rFlac1 is shown in Fig. 5B. With increasing pH from 2.0 to 4.0, the $E°'$ value of rFlac1 shifted to higher potentials and reached the highest value of 0.55 V (vs. Ag|AgCl) at pH 4.0–4.5. With further increasing pH, $E°'$

shifted to lower potentials. A similar pH dependence of $E^{\circ\prime}$ was also observed in our previous study on BOD (17). However, the $E^{\circ\prime}$ value of rFlac1 shifted to lower potentials at a lower pH than that of BOD (rFlac1: pH 4.5, BOD: pH 5.5). In addition, it should be noted that the extent of the negative shift was also larger in rFlac1 (rFlac1: –0.075 V/pH, BOD: –0.050 V/pH). Thus, rFlac1 was found to show a more marked pH dependency of $E^{\circ\prime}$ compared to BOD.

Correlation between the pH dependence of $E^{\circ\prime}$ and the optimum pH of rFlac1

The difference in the formal redox potentials of the enzyme (type 1 copper site) and substrate, $\Delta E^{\circ\prime} = E^{\circ\prime}$(enzyme) – $E^{\circ\prime}$(substrate), was evaluated for three different substrates (ABTS, PPD, and OAP) by using the previous data for $E^{\circ\prime}$ value (substrate) (17). As seen in Fig. 5C, $\Delta E^{\circ\prime}$ reached the highest value at pH 3.5–4.5, 5.5–6.5, and 5.5–6.5, for ABTS, PPD, and OAP, respectively. These pH ranges corresponds well with the optimum pHs for the respective substrates, i.e., 5.0, 5.0, and 6.0–6.5, for ABTS, PPD, and OAP, respectively (arrows in Fig. 5C).

Thus, $\Delta E^{\circ\prime}$ is found to be an important factor that dominantly determines the optimum pH of rFlac1 as previously observed for BOD (17). The $E^{\circ\prime}$ values for rFlac1 were higher than those for BOD in the pH range of 2.0 to 5.5 (0.49–0.55 and 0.45–0.50 for rFlac1 and BOD, respectively). The slope of the pH–$E^{\circ\prime}$ plot in the pH range of 4.5 to 7.0 is steeper for rFlac1 than for BOD, i.e., –0.08 V/pH and –0.03 V/pH for rFlac1 and BOD, respectively. In the case of BOD whose $E^{\circ\prime}$(enzyme) does not show a large dependence on pH, $E^{\circ\prime}$(substrate) should largely contribute to the pH–$\Delta E^{\circ\prime}$ curve.

Accordingly, when ABTS having pH-independent $E^{\circ\prime}$ values is used as substrate, the optimum pH of the enzyme reaction corresponding to the maximum $\Delta E^{\circ\prime}$ is around 4.0, at which the highest $E^{\circ\prime}$(enzyme) value is shown. When PPD and OAP showing the considerably high dependences of $E^{\circ\prime}$ are used, the optimum pH is shifted to neutral to alkaline pHs (e.g., 6.5–8.5 for BOD) from the acidic pH, 4.0 at which the highest $E^{\circ\prime}$(enzyme) value is shown (17). In the case of rFlac1, however, the $E^{\circ\prime}$ value of type 1 copper drastically shifts depending on pH, showing a large pH dependence at pH 4.5–7.0 (Fig. 5B). Accordingly, it can be considered that the contribution from $E^{\circ\prime}$(enzyme) is more dominant than that from $E^{\circ\prime}$ (substrate) to govern the $\Delta E^{\circ\prime}$ value, and the optimum pH is not necessarily highly dependent on substrate. Thus, the unique characteristics of Flac1 with neutral optimum pHs depending on substrates only slightly, could be elucidated in terms of $\Delta E^{\circ\prime}$.

The $E^{\circ\prime}$ value of type 1 copper is determined by its coordination environment. Two His and one Cys are conserved as ligands for type 1 copper in all multi-copper oxidases. A relatively distant axial ligand Met also coordinates the type 1 copper in many multi-copper oxidases such as ascorbate oxidase and BOD. However, the amino acid sequence of Flac1 indicates that a Leu residue is located for the axial Met residue as in many fungal laccases, in which a non-coordinating bulky amino acid such as Leu, Ile, or Phe occupies the axial position so as to inhibit the ligation of the fourth group to type 1 copper. The above three-coordinated enzymes that lost the fourth ligand Met generally show positive $E^{\circ\prime}$ values (27). A decrease in the electron density at the copper atom due to the lack of the Met donor ligand would result in an increase in the

ionization energy and thus give a higher $E^{\circ\prime}$ (38). The replacements of the axial ligand Met to another amino acid residue (39-41) and formation or deletion of hydrogen bonds to ligand groups (42) have resulted in a positive or negative shift of $E^{\circ\prime}$ in multi-copper oxidases. The coordination environment of the type 1 copper site is thus concerned with the $E^{\circ\prime}$ value, however the mechanism of its pH dependence remains unclear.

It is important to mention here that other factors, including the electron transfer rate from type 1 copper to type 2/3 copper cluster and the reduction rate of oxygen to water, are closely concerned with the optimum pH of multi-copper oxidases. In addition to these factors determining the ascending and descending branches of the pH–activity curves, the electron transfer rate from substrate to enzyme would also contribute to the substrate-depending optimum pHs of multi-copper oxidases. Further study is needed to understand the catalytic reaction of multi-copper oxidases more comprehensively.

References

1. **Solomon, E.I., Sundaram, U.M. and Machonkin, T.E.**: Multicopper oxidases and oxygenases, Chem. Rev., **96**, 2563–2605 (1996).

2. **Heinzkill, M., Bech, L., Halkier, T., Schneider, P. and Anke, T.**: Characterization of laccases and peroxidases from wood-rotting fungi (family *Coprinaceae*), Appl. Environ. Microbiol., **64**, 1601–1606 (1998).

3. **Nagai, M., Sato, T., Watanabe, H., Saito, K., Kawata, M. and Enei, H.**: Purification and characterization of an extracellular laccase from the edible mushroom *Lentinula edodes*, and decolorization of chemically different dyes, Appl. Microciol. Biotechnol., **60**, 327–335 (2002).

4. **Kiiskinen, L.L., Viikari, L. and Kruus, K.**: Purification and characterization of a novel laccase from the ascomycete *Melanocarpus albomyces*, Appl. Microbiol. Biotechnol., **59**, 198–204 (2002).

5. **Wahleithner, J.A., Xu, F., Brown, K.M., Brown, S.H., Golightly, E.J., Halkier, T., Kauppinen, S., Pederson, A. and Schneider, P.**: The identification and characterization of four laccases from the plant pathogenic fungus *Rhizoctonia solani*, Curr. Genet., **29**, 395–403 (1996).

6. **Palmieri, G., Giardina, P., Marzullo, L., Desiderio, B., Nitti, G., Cannio, R. and Sannia, G.**: Stability and activity of a phenol oxidase from the ligninolytic fungus *Pleurotus ostreatus*, Appl. Microciol. Biotechnol., **39**, 632–636 (1993).

7. **Min, K.L., Kim, Y.H., Kim, Y.W., Jung, H.S. and Hah, Y.C.**: Characterization of a novel laccase produced by the wood-rotting fungus *Phellinus ribis*, Arch. Biochem.

Biophys., **392**, 279–286 (2001).

8. **Gouka, R.J., van der Heiden, M., Swarthoff, T. and Verrips, C.T.**: Cloning of a phenol oxidase gene from *Acremonium murorum* and its expression in *Aspergillus awamori*, Appl. Environ. Microbiol., **67**, 2610–2616 (2001).

9. **Sulistyaningdyah, W.T., Ogawa, J., Tanaka, H., Maeda, C. and Shimizu, S.**: Characterization of alkaliphilic laccase activity in the culture supernatant of *Myrothecium verrucaria* 24G–4 in comparison with bilirubin oxidase, FEMS Microbiol. Lett., **230**, 209–214 (2004).

10. **Xu, F.**: Effects of redox potential and hydroxide inhibition on the pH activity profile of fungal laccases, J. Biol. Chem., **272**, 924–928 (1997).

11. **Xu, F., Kulys, J.J., Duke, K., Li, K., Krikstopaitis, K, Deussen, H.J., Abbate, E., Galinyte, V. and Schneider, P.**: Redox chemistry in laccase-catalyzed oxidation of N-hydroxy compounds, Appl. Environ. Microbiol., **66**, 2052–2056 (2000).

12. **Kano, K. and Ikeda, T.**: Bioelectrocatalysis, powerful means of connecting electrochemistry to biochemistry and biotechnology, Electrochemistry, **71**, 86–99 (2003).

13. **Tsujimura, S., Nakagawa, T., Kano, K. and Ikeda, T.**: Kinetic study of direct bioelectrocatalysis of dioxygen reduction with bilirubin oxidase at carbon electrodes, Electrochemistry, **72**, 437–439 (2004).

14. **Shleev, S., Jarosz-Wilkolazka, A., Khalunina, A., Morozova, O., Yaropolov, A., Ruzgas, T. and Gorton, L.**: Direct electron transfer reactions of laccases from different origins on carbon electrodes, Bioelectrochemistry, **67**, 115–124 (2005).

15. **Shleev, S., Christenson, A., Serezhenkov, V., Burbaev, D., Yaropolov, A., Gorton, L. and Ruzgas, T.**: Electrochemical redox transformations of T1 and T2 copper sites in native *Trametes hirsuta* laccase at gold electrode, Biochem. J., **385**, 745–754 (2005).

16. **Shleev, S., Kasmi, E.I., Ruzgas, T. and Gorton, L.**: Direct heterogeneous electron transfer reactions of bilirubin oxidase at a spectrographic graphite electrode, Electrochem. Commun., **6,** 934–939 (2004).

17. **Otsuka, K., Sugihara, T., Tsujino, Y., Osakai, T. and Tamiya, E.**: Electrochemical consideration on the optimum pH of bilirubin oxidase, Anal. Biochem., **370**, 98–106 (2007).

18. **Saito (Otsuka), K., Ikeda, R., Endo, K., Tsujino, Y., Takagi, M. and Tamiya, E.**:Isolation of a novel alkali-induced laccase from *Flammulina velutipes* and its application for hair coloring, J. Biosci. Bioeng., **113**, 575–579 (2012).

19. **Kataoka, K., Tanaka, K., Sakai, Y. and Sakurai, T.**: High-level expression of *Myrothecium verrucaria* bilirubin oxidase in *Pichia pastoris*, and its facile purification and characterization, Protein Expr. Purif., **41**, 77–83 (2005).

20. **Yoshida, H.**: Chemistry of laquer (urushi), J. Chem. Soc., **43**, 472–486 (1883).

21. **Messerschmidt, A., Ladenstein, R., Huber, R., Bolognesi, M., Avigliano, L., Petruzzelli, R., Rossi, A. and Finazzi-Agró, A.**: Refined crystal structure of ascorbate oxidase at 1.9 Å resolution, J. Mol. Biol., **224**, 179–205 (1992).

22. **Koikeda, S., Ando, K., Kaji, K., Inoue, T., Murao, S., Takeuchi, K. and Samejima, T.**: Molecular cloning of the gene for bilirubin oxidase from *Myrothecium verrucaria* and its expression in yeast, J. Biol. Chem., **268**, 18801–18809 (1993).

23. **Messerschmidt, A. and Huber, R.**: The blue oxidases, ascorbate oxidase, laccase and ceruloplasmin. Modelling and structural relationships, Eur. J. Biochem., **187**, 341–352 (1990).

24. **Piontek, K., Antorini, M. and Choinowski, T.**: Crystal structure of a laccase from the fungus *Trametes versicolor* at 1.90-Å resolution containing a full complement of coppers, J. Biol. Chem., **277**, 37663–37669 (2002).

25. **Ducros, V., Brzozowski, A.M., Wilson, K.S., Brown, S.H., Ostergaard, P., Schneider, P., Yaver, D.S., Pedersen, A.H. and Davies, G.J.**: Crystal structure of the type-2 Cu depleted laccase from *Coprinus cinereus* at 2.2 Å resolution, Nat. Struct. Biol., **5**, 310–316 (1998).

26. **Gavel, Y. and Von Heijne, G.**: Sequence differences between glycosylated and non-glycosylated Asn-X-Thr/Ser acceptor sites: implications for protein engineering, Protein Eng., **3**, 433–442 (1990).

27. **Xu, F., Shin, W., Brown, S.H., Wahleithner, J.A., Sundaram, U.M. and Solomon, E.I.**: A study of a series of recombinant fungal laccases and bilirubin oxidase that exhibit significant differences in redox potential, substrate specificity, and stability, Biochim. Biophys. Acta, **1292**, 303–311 (1996).

28. **Sakurai, T. and Kataoka, K.**: Multi-copper proteins, p. 131–168. in Karlin, K. and Ito, S. (ed.), Copper Oxygen Chemistry, John Wiley & Sons Inc, Hoboken, (2011).

29. **Jönsson, L.J., Saloheimo, M. and Penttilä M.**: Laccase from the white-rot fungus *Trametes versicolor*: cDNA cloning of *lcc1* and expression in *Pichia pastoris*, Curr. Genet., **32**, 425–430 (1997).

30. **Soden, D.M., O'Callaghan, J. and Dobson, A.D.**: Molecular cloning of a laccase isozyme gene from *Pleurotus sajor-caju* and expression in the heterologous *Pichia pastoris* host, Mycrobiology, **148**, 4003–4014 (2002).

31. **Sakurai, T., Sawada, S., Suzuki, S. and Nakahara, A.**: Oxidation of reduced cucumber ascorbate oxidase, Biochem. Biophys. Res. Commun., **131**, 647–652 (1985).

32. **Samejima, T., Wu, C.S., Shiboya, K., Kaji, H., Koikeda, S., Ando, K. and Yang, J.T.**: Conformation of bilirubin oxidase in native and denatured states, J. Protein Chem., **13**, 307–13 (1994).

33. **Kataoka, K., Kitagawa, R., Inoue, M., Naruse, D., Sakurai, T. and Huang, H.**: Point mutations at the type I Cu ligands, Cys457 and Met467, and at the putative proton donor, Asp105, in *Myrothecium verrucaria* bilirubin oxidase and reactions with dioxygen, Biochemistry, **44**, 7004–7012 (2005).

34. **Garzillo, A.M., Colao, M.C., Buonocore, V., Oliva, R., Falcigno, L., Saviano, M., Santoro, A.M., Zappala, R., Bonomo, R.P., Bianco, C., Giardina, P., Palmieri, G. and Sannia, G.**: Structural and kinetic characterization of native laccases from *Pleurotus ostreatus*, *Rigidoporus lignosus*, and *Trametes trogii*, J. Protein Chem., **20**, 191–201 (2001).

35. **Huang, H., Zoppellaro, G., and Sakurai, T.**: Spectroscopic and kinetic studies on the oxygen-centered radical formed during four-electron reduction process of dioxygen by *Rhus verinicifera* laccase, J. Biol. Chem., **274**, 32718-32724 (1999).

36. **Kataoka, K., Sugiyama, R., Hirota, S., Inoue, M., Urata, K., Minagawa, Y., Seo, D., and Sakurai, T.**: Four-electron reduction of dioxygen by a multicopper oxidase,

CueO, and roles of Asp112 and Glu506 located adjacent to the trinuclear copper center, J. Biol. Chem., **284**, 11405-14413 (2009).

37. **Kamitaka, Y., Tsujimura, S. and Kano, K.**: High current density bioelectrolysis of D-fructose at fructose dehydrogenase-adsorbed and Ketjen black-modified electrodes without a mediator, Chem. Lett., **36**, 218–219 (2007).

38. **Guckert, J.A., Lowery, M.D. and Solomon, E.I.**: Electronic structure of the reduced blue copper active site: contributions to reduction potentials and geometry, J. Am. Chem. Soc., **117**, 2817–2844 (1995).

39. **Karlsson, B.G., Aasa, R., Malmström, B.G. and Lundberg, L.G.**: Rack-induced bonding in blue copper proteins: spectroscopic properties and reduction potential of the azurin mutant Met-121 → Leu, FEBS Lett., **253**, 99–102 (1989).

40. **Kamitaka, Y., Tsujimura, S., Kataoka, K., Sakurai, T., Ikeda, T. and Kano, K.**: Effects of axial ligand mutation of the type I copper site in bilirubin oxidase on direct electron transfer-type bioelectrocatalytic reduction of dioxygen, J. Electroanal. Chem., **601**, 119–124 (2007).

41. **Kurose, S., Kataoka, K., Shinohara, N., Miura, Y., Tsutsumi, M., Tsujimura, S., Kano, K. and Sakurai, T.**: Modification of spectroscopic properties and catalytic activity of *Escherichia coli* CueO by mutations of methionine 510, the axial ligand to the type I Cu, Bull. Chem. Soc. Jpn., **82**, 504–508 (2009).

42. **Kataoka, K., Hirota, S., Maeda, Y., Kogi, H., Shinohara, N., Sekimoto, M. and Sakurai, T.**: Enhancement of laccase activity through the construction and breakdown of a hydrogen bond at the type I copper center in *Escherichia coli* CueO and the

deletion mutant Δα5-7 CueO, Biochemistry, **50**, 558–565 (2011).

Figure legends

Fig. 1. (A) cDNA sequence and deduced amino acid sequence of Flac1 (AB253791). cDNA corresponded with the mature Flac1 was 1491 bp from 5'-terminus. Double line indicates the copper binding sites, His395, Cys451, and His456 for type 1 copper, His64 and His398 for type 2 copper and His66, His109, His111, His400, His450, and His452 for type 3 coppers. Single under line shows the *N*-glycosilation site. The disulphide bridges are indicated as dashed-line between 2 cysteines. Stop codon is denoted by asterisk. Box is *Not* Ⅰ -d$(T)_{18}$ primer. (B) Alignment of amino acid sequence around the metal binding sites in multi-copper oxidase: ChLc, *Tramtes* (*Coriolus) hirsutus* laccase [AAL89554]; TvLc, *Trametes versicolor* laccase [CAA59161]; PoLc, *Pleurotus ostreatus* diphenol oxidase [CAA84357]; RvLc, *Rhus vernicifera* laccase [BAB63411]; AOX, ascorbate oxidase from zucchini; BOD, *Myrothecium verrucaria* bilirubin oxidase [BAA03166]; hCp, *human* ceruloplasmin; CueO, CueO from *E. coli* [1KV7A]; Fet3p, Fet3p from Saccharomyces cerevisiae [1ZPU], and CopA, CopA from *Pseudomonas syringe* [P12374]. The amino acids involved in the binding to copper ions are indicated by asterisks and the types of copper by Arabic numbers.

Fig. 2. (A) Absorption, (B) CD, and (C) ESR spectra of rFlac1. Measurements conditions: (A) 0.1 M potassium phosphate buffer (pH 7.0) at room temperature; (B) 0.1 M potassium phosphate buffer (pH 7.0) at room temperature; sensitivity 2.0 m°/cm; time constant, 2 s; scan speed, 20 nm/min (C) temperature, 77 K; power, 5.0 mW; frequency, 9.193 GHz; modulation, 100 kHz and 1.0 mT; amplitude, 790; filter, 0.1s;

sweep time, 8 min.

Fig. 3. pH dependencies of the oxidase activities of rFlac1 for ABTS (filled circles), PPD (open triangles), and OAP (filled diamonds). A MES-Tris-sodium acetate buffer was used.

Fig. 4. (A) Cyclic voltammograms recorded with the KB modified HOPG electrode (a) with and (b) without the adsorption of rFlac1 on the electrode surface at pH 5.0. Dashed line indicates the base current corrected for the effect of enzyme adsorption by multiplying the base current with an appropriate factor (= 0.85 in this case). Scan rate: 0.02 V s^{-1}. (B) The base current-corrected cyclic voltammogram of rFlac1 at pH 5.0. (C) Cyclic voltammograms (not corrected for the base currents) recorded with the KB modified HOPG electrode with the adsorption of rFlac1 at pH 3.0, 5.0, and 7.0. Scan rate: 0.02 V s^{-1}.

Fig. 5. (A) Base current-corrected steady-state linear sweep voltammograms recorded with the KB modified HOPG electrode with the adsorption of rFlac1 at pH 5.0. Open squares represent the theoretical values obtained by a non-linear regression analysis with Eqs. (1)–(3). Scan rate: 0.02 V s^{-1}. (B) The pH dependence of $E^{\circ\prime}$ for rFlac1. (C) Plots of $\Delta E^{\circ\prime}$ ($\Delta E^{\circ\prime} = E^{\circ\prime}$(enzyme, type 1 copper)– $E^{\circ\prime}$(substrates)) against pH for ABTS (filled circle), PPD (open triangle), and OAP (filled diamond). The $E^{\circ\prime}$ values for ABTS, PPD, and OAP were cited from the previous report (17). Arrows indicate the

optimum pHs of rFlac1 for ABTS (5.0), PPD (5.0) and OAP (6.0–6.5).

Table 1. The values of $k°$, α, Γ_t, $E°'$, and σ obtained from the regression analysis for the-DET-type rFlac1-catalyzed O_2 reduction wave at the KB modified HOPG electrode.

pH	$k°/s^{-1}$	α	$\Gamma_t/10^{-12}$ mol cm^{-2} [a]	$E°'$/V vs. Ag|AgCl|KCl$_{sat}$	σ[b]/μA cm^{-2}
2.0	68	0.24	2.5	0.53	1.78
2.5	78	0.18	1.8	0.53	1.01
3.0	85	0.15	3.1	0.54	1.21
3.5	49	0.23	3.9	0.55	1.81
4.0	40	0.24	4.3	0.55	1.42
4.5	42	0.27	3.2	0.55	1.09
5.0	110	0.20	5.3	0.52	2.54
5.5	95	0.15	2.0	0.49	2.30
6.0	120	0.18	1.7	0.44	2.17
6.5	90	0.20	1.0	0.43	1.83
7.0	50	0.10	2.7	0.36	2.64

[a] Estimated using the geometric area of the electrode surface.

[b] Standard deviation $\sigma = [\sum(i_{calcd} - i_{obsd})^2/(N\text{-}1)]^{1/2}$, i_{calcd}: current density obtained by the non-linear regression analysis with Eqs. (1)–(3), i_{obsd}: current density observed at the KB modified HOPG electrode absorbing rFlac1, N: the number of data points (i.e., 700).

Fig. 1. (A)

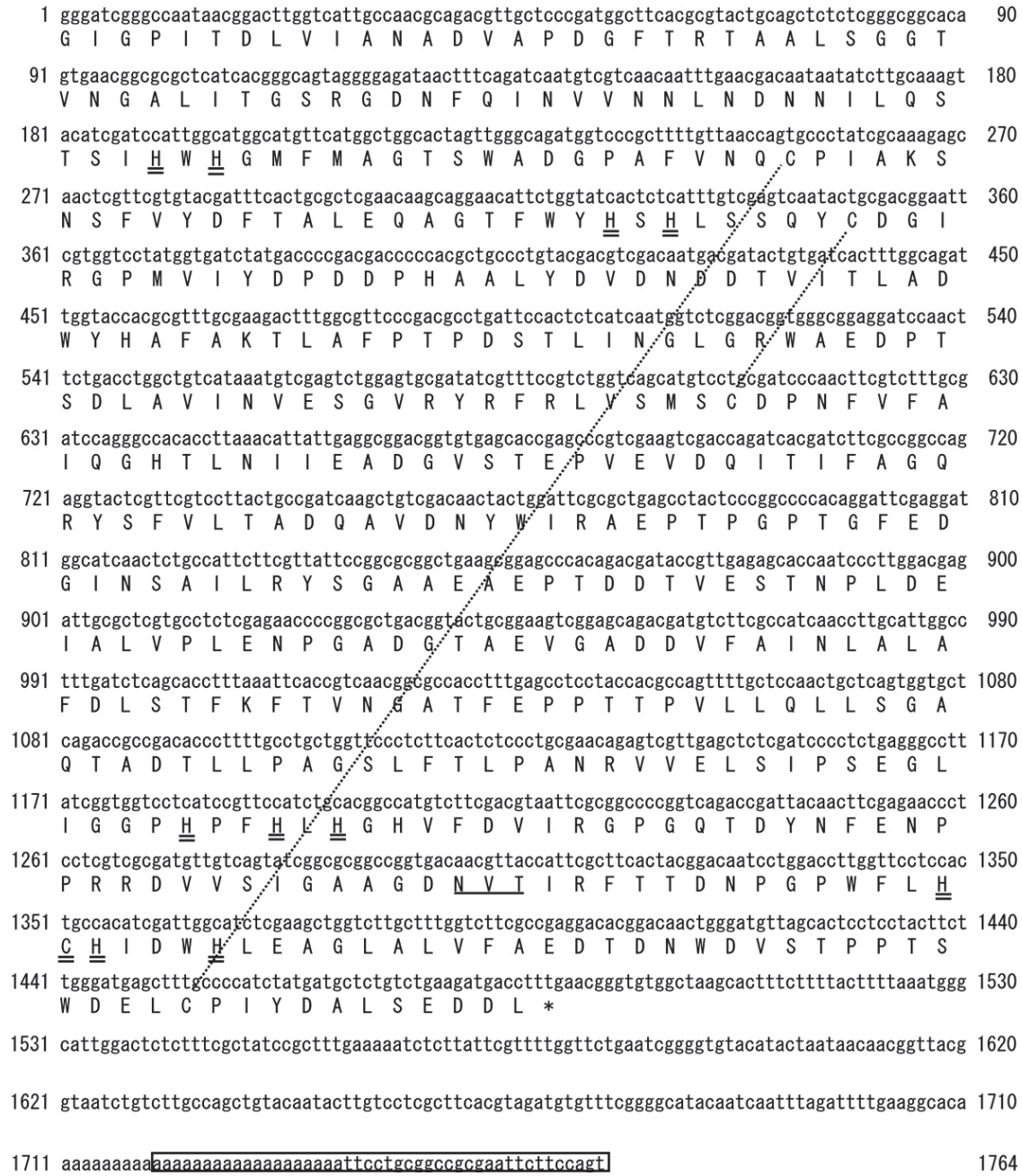
1 gggatcgggccaataacggacttggtcattgccaacgcagacgttgctcccgatggcttcacgcgtactgcagctctctcgggcggcaca 90
G I G P I T D L V I A N A D V A P D G F T R T A A L S G G T
91 gtgaacggcgcgctcatcacgggcagtaggggagataactttcagatcaatgtcgtcaacaatttgaacgacaataatatcttgcaaagt 180
V N G A L I T G S R G D N F Q I N V V N N L N D N N I L Q S
181 acatcgatccattggcatggcatgttcatggctggcactagttgggcagatggtcccgcttttgttaaccagtgccctatcgcaaagagc 270
T S I H W H G M F M A G T S W A D G P A F V N Q C P I A K S
271 aactcgttcgtgtacgatttcactgcgctcgaacaagcaggaacattctggtatcactctcatttgtcgagtcaatactgcgacggaatt 360
N S F V Y D F T A L E Q A G T F W Y H S H L S S Q Y C D G I
361 cgtggtcctatggtgatctatgaccccgacgacccccacgctgccctgtacgacgtcgacaatgacgatactgtgatcactttggcagat 450
R G P M V I Y D P D D P H A A L Y D V D N D D T V I T L A D
451 tggtaccacgcgtttgcgaagactttggcgttcccgacgcctgattccactctcatcaatggtctcggacggtgggcggaggatccaact 540
W Y H A F A K T L A F P T P D S T L I N G L G R W A E D P T
541 tctgacctggctgtcataaatgtcgagtctggagtgcgatatcgtttccgtctggtcagcatgtcctgcgatcccaacttcgtctttgcg 630
S D L A V I N V E S G V R Y R F R L V S M S C D P N F V F A
631 atccagggccacaccttaaacattattgaggcggacggtgtgagcaccgagccgtcgaagtcgaccagatcacgatcttcgccggccag 720
I Q G H T L N I I E A D G V S T E P V E V D Q I T I F A G Q
721 aggtactcgttcgtccttactgccgatcaagctgtcgacaactactggattcgcgctgagcctactcccggccccacaggattcgaggat 810
R Y S F V L T A D Q A V D N Y W I R A E P T P G P T G F E D
811 ggcatcaactctgccattcttcgttattccggcgcggctgaaggcggagcccacagacgataccgttgagagcaccaatcccttggacgag 900
G I N S A I L R Y S G A A E A E P T D D T V E S T N P L D E
901 attgcgctcgtgcctctcgagaaccccggcgctgacggtactgcggaagtcggagcagacgatgtcttcgccatcaaccttgcattggcc 990
I A L V P L E N P G A D G T A E V G A D D V F A I N L A L A
991 tttgatctcagcacctttaaattcaccgtcaacggcgccaccttgagcctcctaccacgccagttttgctccaactgctcagtggtgct 1080
F D L S T F K F T V N G A T F E P P T T P V L L Q L L S G A
1081 cagaccgccgacaccctttgcctgctggttcctcttcactctccctgcgaacagagtcgttgagctctcgatcccctctgagggcctt 1170
Q T A D T L L P A G S L F T L P A N R V V E L S I P S E G L
1171 atcggtggtcctcatccgttccatctgcacggccatgtcttcgacgtaattcgcggccccggtcagaccgattacaacttcgagaaccct 1260
I G G P H P F H L H G H V F D V I R G P G Q T D Y N F E N P
1261 cctcgtcgcgatgttgtcagtatcggcgcggccggtgacaacgttaccattcgcttcactacggacaatcctggaccttggttcctccac 1350
P R R D V V S I G A A G D N V T I R F T T D N P G P W F L H
1351 tgccacatcgattggcatctcgaagctggtcttgctttggtcttcgccgaggacacggacaactgggatgttagcactcctcctacttct 1440
C H I D W H L E A G L A L V F A E D T D N W D V S T P P T S
1441 tgggatgagctttgccccatctatgatgctctgtctgaagatgacctttgaacgggtgtggctaagcactttcttttacttttaaatggg 1530
W D E L C P I Y D A L S E D D L *
1531 cattggactctctttcgctatccgctttgaaaaatctcttattcgttttggttctgaatcggggtgtacatactaataacaacggttacg 1620
1621 gtaatctgtcttgccagctgtacaatacttgtcctcgcttcacgtagatgtgtttcggggcatacaatcaatttagattttgaaggcaca 1710
1711 aaaaaaaaaaaaaaaaaaaaaaaaaaaattcctgcggccgcgaattcttccagt 1764

Fig. 1. (B)

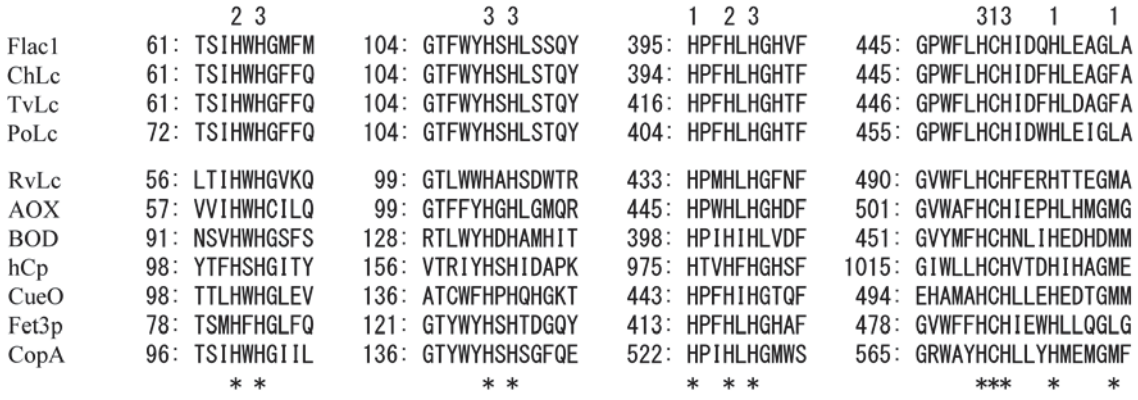
2 3
3 3
1 2 3
313 1 1
Flac1 61: TSIHWHGMFM 104: GTFWYHSHLSSQY 395: HPFHLHGHVF 445: GPWFLHCHIDQHLEAGLA
ChLc 61: TSIHWHGFFQ 104: GTFWYHSHLSTQY 394: HPFHLHGHTF 445: GPWFLHCHIDFHLEAGFA
TvLc 61: TSIHWHGFFQ 104: GTFWYHSHLSTQY 416: HPFHLHGHTF 446: GPWFLHCHIDFHLDAGFA
PoLc 72: TSIHWHGFFQ 104: GTFWYHSHLSTQY 404: HPFHLHGHTF 455: GPWFLHCHIDWHLEIGLA
RvLc 56: LTIHWHGVKQ 99: GTLWWHAHSDWTR 433: HPMHLHGFNF 490: GVWFLHCHFERHTTEGMA
AOX 57: VVIHWHCILQ 99: GTFFYHGHLGMQR 445: HPWHLHGHDF 501: GVWAFHCHIEPHLHMGMG
BOD 91: NSVHWHGSFS 128: RTLWYHDHAMHIT 398: HPIHIHLVDF 451: GVYMFHCHNLIHEDHDMM
hCp 98: YTFHSHGITY 156: VTRIYHSHIDAPK 975: HTVHFHGHSF 1015: GIWLLHCHVTDHIHAGME
CueO 98: TTLHWHGLEV 136: ATCWFHPHQHGKT 443: HPFHIHGTQF 494: EHAMAHCHLLEHEDTGMM
Fet3p 78: TSMHFHGLFQ 121: GTYWYHSHTDGQY 413: HPFHLHGHAF 478: GVWFFHCHIEWHLLQGLG
CopA 96: TSIHWHGIIL 136: GTYWYHSHSGFQE 522: HPIHLHGMWS 565: GRWAYHCHLLYHMEMGMF
* *
* *
* * *
*** * *

Fig. 2.

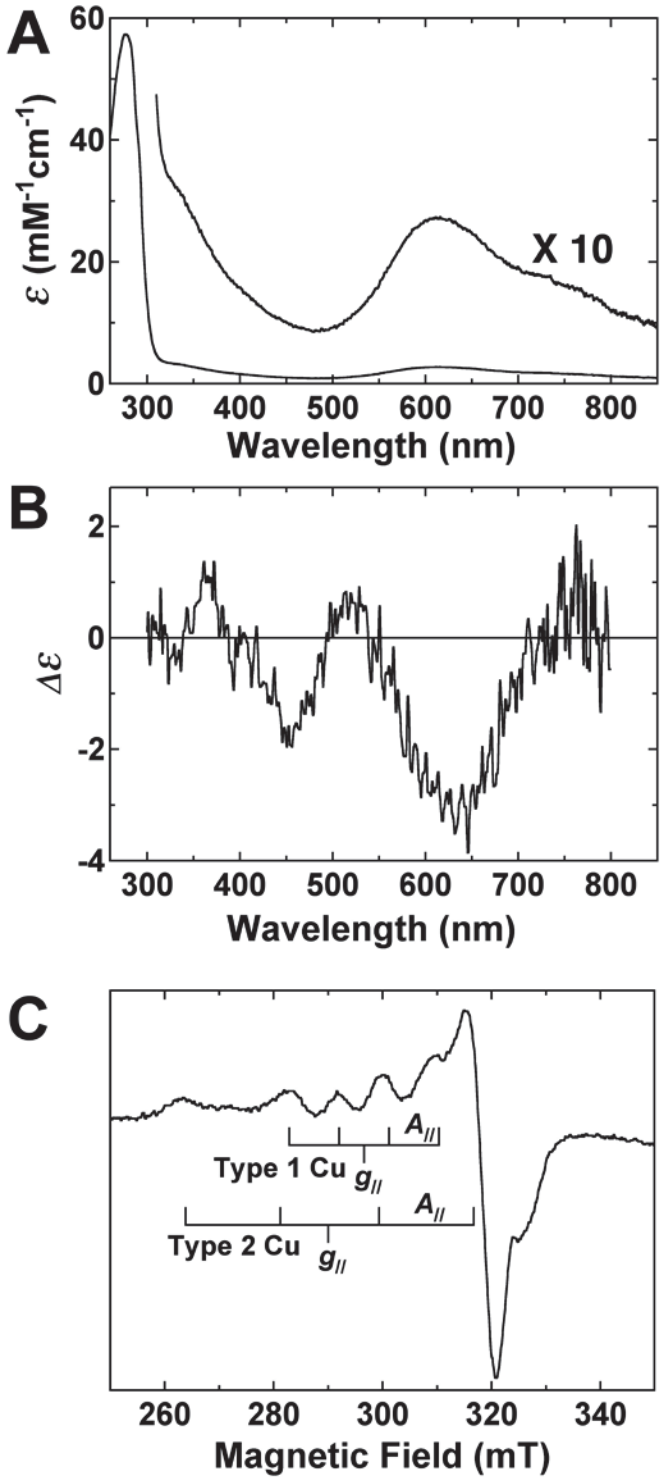
A
60
40
20
0
ε (mM-1cm-1)
X 10
300
400
500
600
700
800
Wavelength (nm)
B
2
0
-2
-4
Δε
300
400
500
600
700
800
Wavelength (nm)
C
A//
Type 1 Cu g//
A//
Type 2 Cu g//
260
280
300
320
340
Magnetic Field (mT)

Fig. 3.

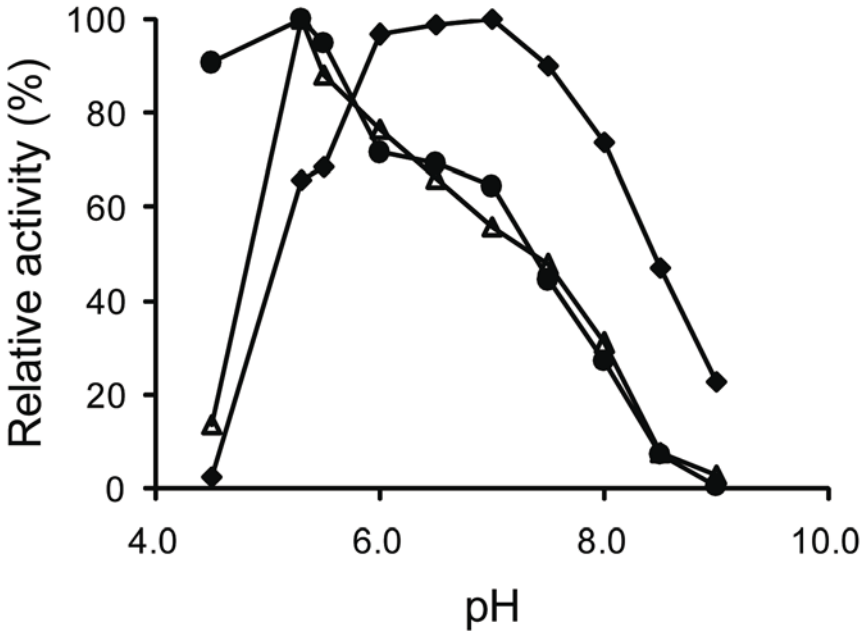

Fig. 4.

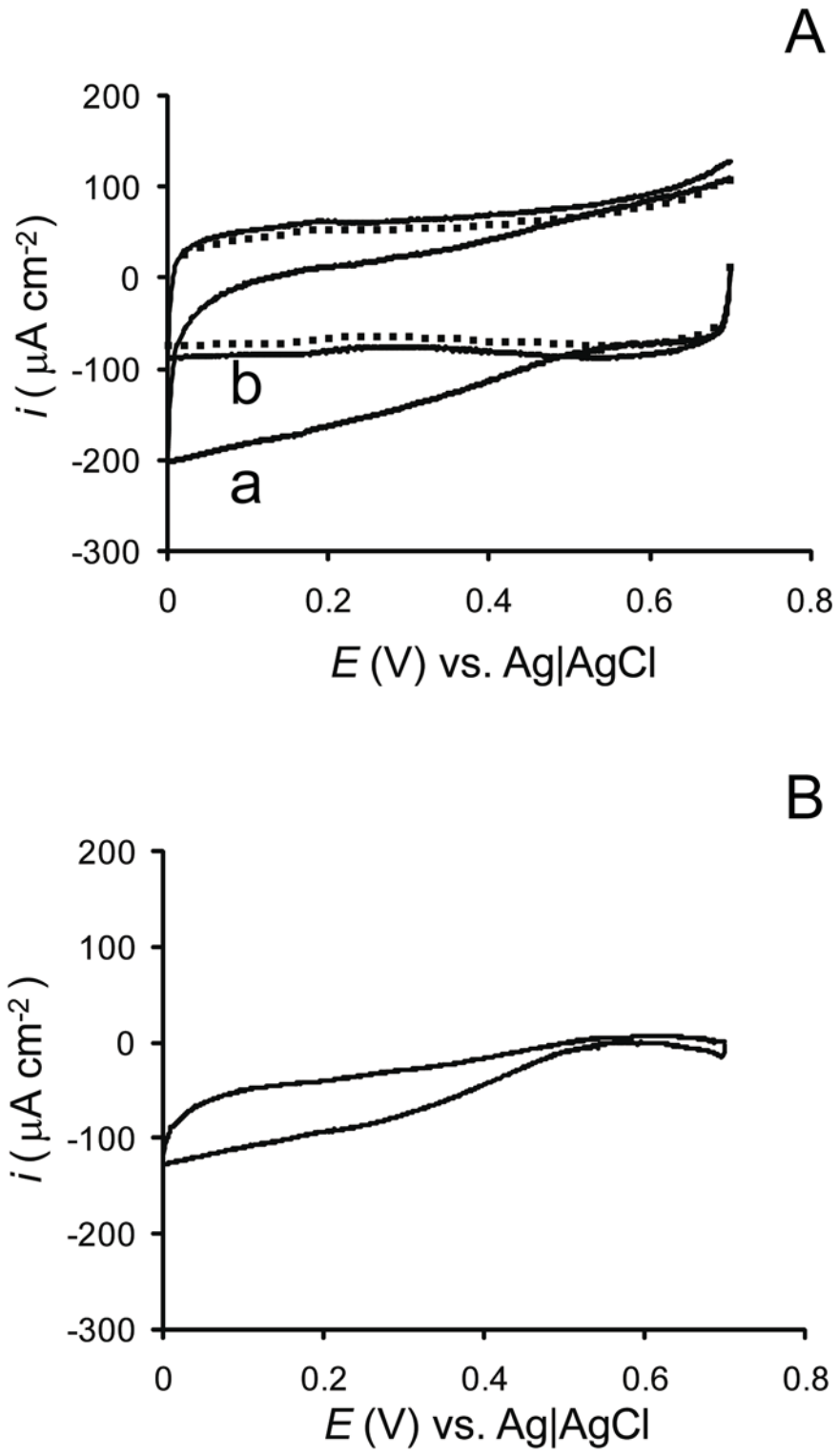
A
200
100
0
-100
-200
-300
i (μA cm-2)
b
a
0
0.2
0.4
0.6
0.8
E (V) vs. Ag|AgCl
B
200
100
0
-100
-200
-300
i (μA cm-2)
0
0.2
0.4
0.6
0.8
E (V) vs. Ag|AgCl

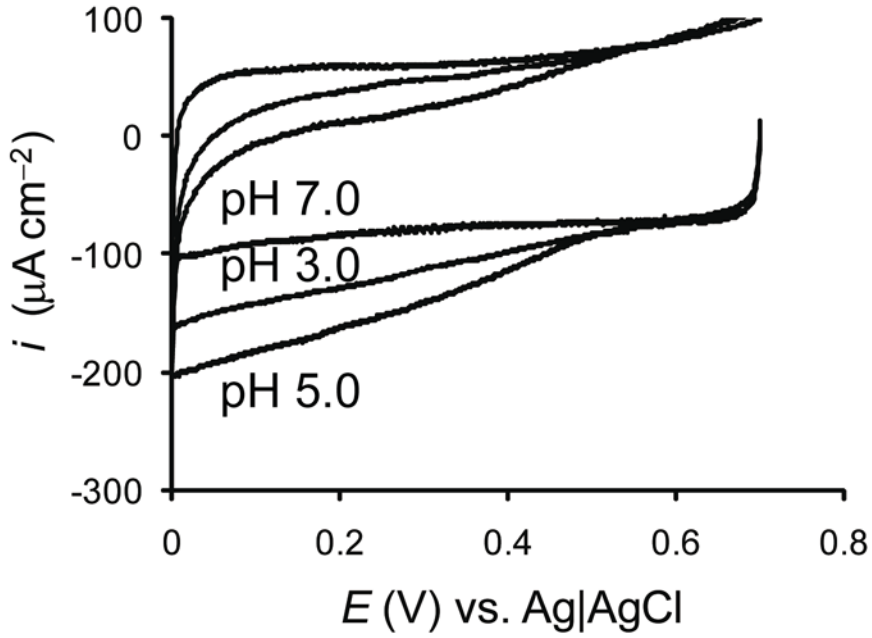
100
0
-100
-200
-300
0
0.2
0.4
0.6
0.8
i (μA cm−2)
E (V) vs. Ag|AgCl
pH 7.0
pH 3.0
pH 5.0

Fig. 5.

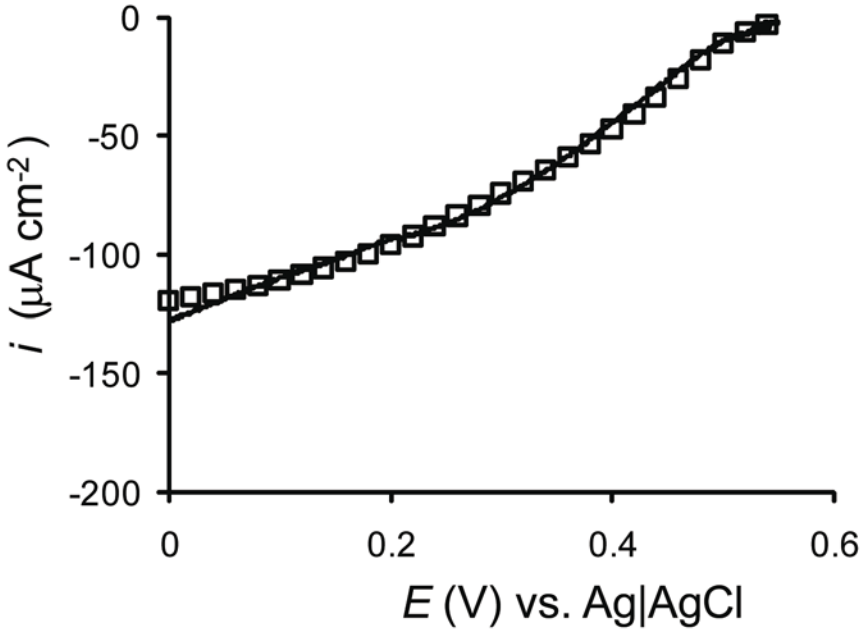

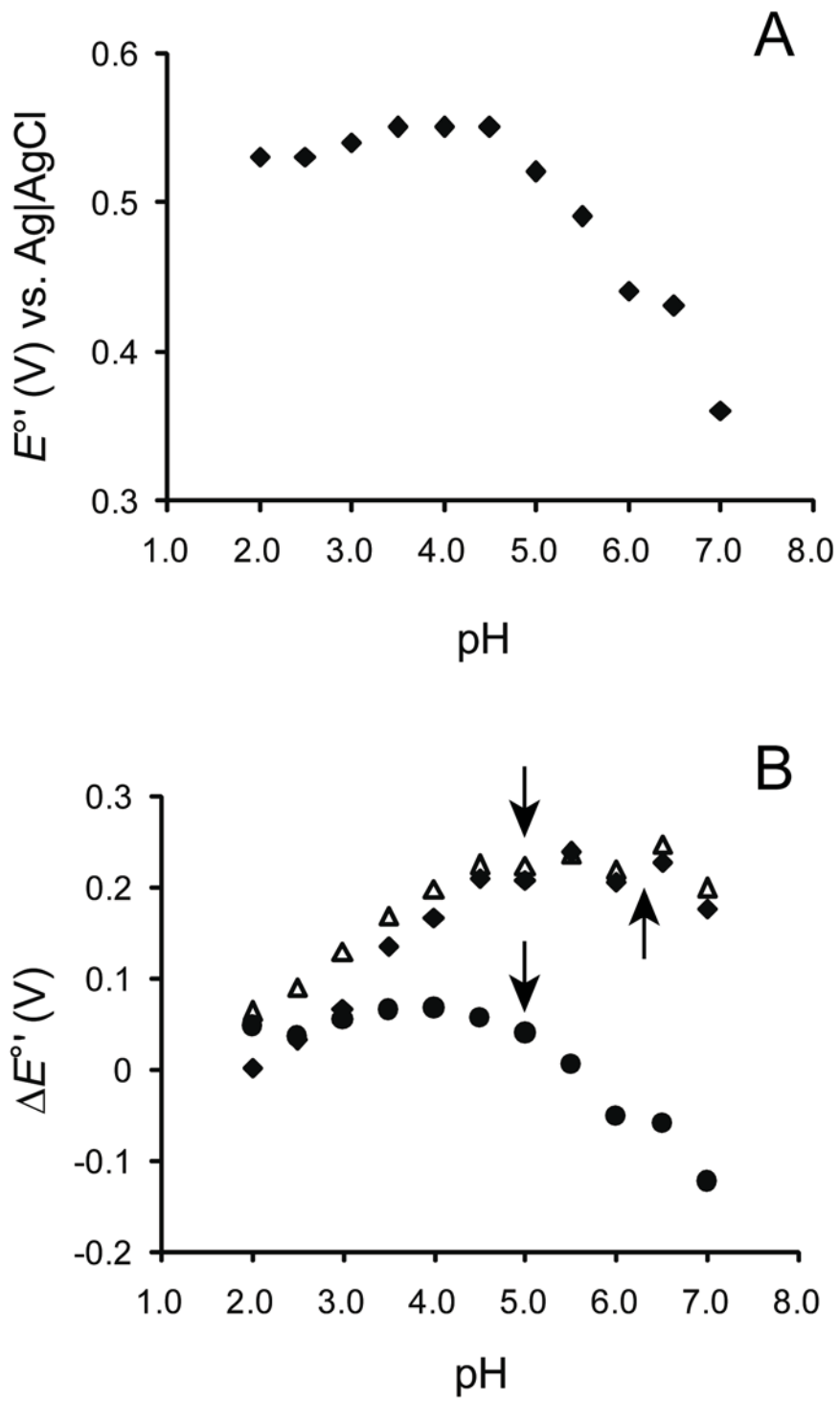
A
0.6
0.5
0.4
0.3
E°' (V) vs. Ag|AgCl
1.0
2.0
3.0
4.0
5.0
6.0
7.0
8.0
pH
B
0.3
0.2
0.1
0
-0.1
-0.2
ΔE°' (V)
1.0
2.0
3.0
4.0
5.0
6.0
7.0
8.0
pH